

**Contribution of Extragalactic Infrared Sources to  
CMB Foreground Anisotropy**

Eric Gawiser and George F. Smoot

Department of Physics and Lawrence Berkeley National Laboratory, University of  
California, Berkeley, Berkeley, CA 94720

Received \_\_\_\_\_; accepted \_\_\_\_\_

## ABSTRACT

We estimate the level of confusion of Cosmic Microwave Background (CMB) anisotropy measurements caused by extragalactic infrared sources. CMB anisotropy observations at high resolution and high frequencies are especially sensitive to this foreground. We have combined IRAS data on bright infrared galaxies with information about the Galaxy from the DIRBE and FIRAS instruments of COBE. Using the spectrum of the Milky Way as a template, we predict the microwave emission of the 5319 brightest infrared galaxies. We simulate skymaps of extragalactic infrared sources over the relevant range of frequencies (30-900 GHz) and instrument resolutions ( $10'$  –  $10^\circ$  Full Width Half Max). Analysis of the temperature anisotropy of these skymaps shows a level of extragalactic infrared foreground that is nearly consistent with previous estimates based on galaxy-evolution models. A reasonable observational window is still available for medium- and small-angular scale CMB anisotropy measurements.

*Subject headings:* cosmic microwave background: data analysis, foregrounds – infrared galaxies – infrared sources: extragalactic

## 1. Introduction

The COBE detection of large-angular scale Cosmic Microwave Background anisotropy (Smoot et al. 1992) has led to tremendous interest in measuring CMB anisotropy on all angular scales with the goal of determining several important cosmological parameters. Current anisotropy observations focus on sub-degree angular scales which correspond to observable structures in the present universe. With improved instrumentation and the promise of a new satellite mission, angular scales between one-half and one-sixth of a degree will be the focus in the next decade.

Due to its large beam size, COBE was basically unaffected by extragalactic foreground sources (Banday et al. 1996, Kogut et al. 1994). Because the contribution of a point source increases with the inverse square of the beam size ( $1/\text{solid angle}$ ), observations at higher angular resolution are more sensitive to extragalactic foregrounds, including infrared-bright galaxies, radio sources, and the Sunyaev-Zel'dovich effect from galaxy clusters. High resolution CMB anisotropy measurements typically use higher frequencies than large-angular scale observations, making far-infrared foregrounds a greater concern. This paper examines the extragalactic infrared sources which contribute to apparent CMB anisotropy.

Previous work in this area (Toffolatti et al. 1994, Francheschini et al. 1989, Wang 1991) used galactic evolution models with specific assumptions about dust temperatures to predict the level of extragalactic foreground. We choose a phenomenological approach using the far-infrared sources detected by the Infrared Astronomical Satellite (IRAS). The IRAS 1.2 Jy catalog (Fisher et al. 1995) provides flux measurements of 5319 external galaxies at 12, 25, 60, and 100  $\mu\text{m}$ , where galactic emission arises mainly from interstellar dust. Each IRAS 1.2 Jy source is fit to measurements of the total Galactic flux made by the DIRBE (Diffuse Infrared Background Experiment) instrument on COBE. We then use the

dust emission spectrum of the Milky Way measured by FIRAS (the Far-Infrared Absolute Spectrophotometer) to extrapolate each IRAS galaxy to the frequencies between 30 and 900 GHz used by CMB anisotropy experiments.

The FIRAS instrument has accumulated evidence for the existence of Cold ( $< 15\text{K}$ ) Dust in the plane of our galaxy (Reach et al. 1995). There is every reason to suspect that if the Milky Way has Cold Dust, then so do other dusty spirals, which comprise the majority of bright extragalactic infrared sources. Some observations (Chini et al. 1995, Block et al. 1994, Devereux & Young 1992) indicate the presence of Cold Dust in other galaxies. Dust this close in temperature to the 2.73 K background radiation could confuse our attempts to separate the Galactic and extragalactic infrared foregrounds from CMB anisotropies. Instead of making specific assumptions about the temperature and optical depth of Cold Dust, we rely on the FIRAS spectrum of our Galaxy to include the microwave emission from all Galactic dust components.

To simulate balloon and satellite observation, we convolve all sources on pixelized skymaps (2X oversampled) of resolution varying from  $10'$  to  $10^\circ$ . The resulting maps covering a range of frequencies from 30 to 900 GHz are analyzed to determine the expected contribution of IRAS galaxies to foreground confusion of CMB temperature anisotropy. The information contained in these skymaps can be used by satellite and balloon missions to choose frequencies and regions of the sky in which to observe (Smoot et al. 1995).

## 2. Extragalactic Infrared Sources

The far-infrared discrete sources detected by IRAS are typically inactive spiral galaxies, although some are quasars, starburst galaxies, and Seyfert galaxies. The IRAS 1.2 Jy catalog contains the 5321 brightest IRAS point sources which have been identified as

external galaxies. The fluxes in this catalog are more carefully analyzed than those in the full IRAS Point Source Catalog. When the locations of these galaxies are compared with those of the thousand brightest radio sources, only 7 possible coincidences result. This lack of coincidence shows that radio-loud galaxies can be handled separately. We perform our analysis after removing the Large and Small Magellanic Clouds, which are resolved by IRAS and DIRBE and have large integrated fluxes. The remaining 5319 sources are roughly isotropic in distribution, except for a clear pattern of the Supergalactic Plane. The 1.2 Jy catalog contains no sources within  $5^\circ$  of the galactic plane or in the other 2% of the sky not scanned by IRAS. There are slightly fewer sources, resulting in a smaller contribution to measured CMB anisotropy, in the regions near the galactic plane, probably due to extinction by Galactic dust. To avoid underestimating the anisotropy and to reduce the possibility of residual galactic contamination, we use a skymap in our analysis that covers galactic latitudes  $|b| > 30^\circ$ . We map 2979 galaxies for a  $0.5^\circ$  beam.

The nature of dust in spiral galaxies is still an open question. It seems likely that there is dust at widely varying temperatures and possibly with different emissivities (Rowan-Robinson 1992, Franceschini & Andreani 1995). Attempts to fit observational data have yielded a variety of results; it is unclear if far-infrared luminous dust is well described by a one-component or a two-component model, and the emissivity power-law index is only known to be between 1 and 2. We avoid specifying the nature of this dust by using DIRBE and FIRAS observations of the spectrum of the Milky Way and by assuming that IRAS galaxies are similar. In fact, fitting a two-component dust model to all IRAS galaxies and to the integrated DIRBE 12, 25, 60, and  $100 \mu\text{m}$  fluxes of the Milky Way produces similar results for the Warm (15-40 K) Dust component to which IRAS and DIRBE are most sensitive. For an emissivity power-law index of 1.5, DIRBE gives a Warm Dust temperature of 28K for the Milky Way, while the 425 IRAS galaxies with highest-quality flux measurements are collectively fit to a Warm Dust temperature of 33K. This Warm

Dust accounts for the majority of the far-infrared emission of spiral galaxies.

There is observational evidence that the far-infrared emission of inactive spirals is dominated by dust slightly colder than 20K (Neininger & Guelin 1996, Chini & Krugel 1993), which seems in conflict with the above fit to bright IRAS galaxies. Fitting the FIRAS spectrum of the Milky Way also leads to a Warm Dust temperature close to 20K, which similarly appears to conflict with the fit to DIRBE Galactic fluxes up to 100  $\mu\text{m}$ . Using 60, 100, 140, and 240  $\mu\text{m}$  DIRBE fluxes, however, indicates a Warm Dust temperature for the Galaxy of 24K. This shows that temperature fits to data on one side of the peak of the assumed blackbody spectrum can be inaccurate. Figure 1 shows that the spectra of the Milky Way found by DIRBE and FIRAS are indeed compatible. It may be an oversimplification to represent the Warm Dust in a galaxy by a single temperature. In fitting each IRAS 1.2 Jy source to the DIRBE fluxes of the Milky Way, we give more weight to the 60 and 100  $\mu\text{m}$  fluxes, which are most sensitive to Warm Dust, than to the 12 and 25  $\mu\text{m}$  fluxes, which are also sensitive to Hot (100-300 K) Dust. For each source, we use only those fluxes given the highest available level of confidence in the 1.2 Jy catalog.

We recognize that not all IRAS galaxies have exactly the same far-IR spectrum as the Milky Way. Active galaxies are warmer, but cannot easily be distinguished from inactive spirals based upon their IRAS colors. Franceschini & Andreani (1995) used observations at 1.25 mm to determine that the Galaxy is similar to inactive spirals in some characteristics but may be similar to starburst galaxies in others. Some observations indicate that our Galaxy is slightly warmer than the average inactive spiral (Chini et al. 1995). These concerns make the Milky Way a good middle-of-the-road choice, and the DIRBE-based dust temperature fits given above agree with the average IRAS galaxy fit rather well. It would be advantageous to use the Milky Way as a template only for known inactive spirals and to fit other morphological types to an appropriate far-IR to microwave spectrum. Unfortunately,

no trustworthy template spectrum is currently available for active galaxies, so the DIRBE and FIRAS measurements of the Milky Way are the best option. Our Galactic spectrum agrees well with observed correlations between radio and IR fluxes of IRAS galaxies (Condon & Broderick 1991, Crawford et al. 1995), supporting our assumption that IRAS 1.2 Jy sources will have a common microwave spectrum.

After removing Galactic emission lines (as in Reach et al. 1995), we fit a smooth curve to the dust spectrum measured by FIRAS. It is possible to vary the parameters of the dust model significantly and still have an acceptable fit, so we refrain from giving any physical importance to the parameters of the fit. Our fit has similar dust temperatures to those of Reach et al. (1995), but we find an optical depth of the 4K Cold Dust component twelve times that of the 19K Warm Dust component whereas their 8 K Cold Dust has seven times the optical depth of the Warm Dust. This difference appears to be due to using different emissivity functions and serves as a warning that noticeably different models can fit the FIRAS spectrum rather well, making extrapolation of dust emission beyond the end of the FIRAS spectrum dangerous. We add synchrotron and free-free components with microwave-range spectral indices of  $-1.0$  and  $-0.15$ , respectively, such that these sources of microwave emission match the observations of COBE (Kogut et al. 1996, Reach et al. 1995, Bennett et al. 1992) below 100 GHz. Free-free emission is stronger than dust beyond the low-frequency end of the FIRAS spectrum.

We combine this FIRAS curve with DIRBE data to form the broad Galactic spectrum shown in Figure 1. Each IRAS source is fit to the DIRBE end of the spectrum and extrapolated to the desired frequency using the FIRAS curve. This approach contrasts with previous work because we use observational data to create a spectrum for the extrapolation of extragalactic infrared sources to microwave frequencies rather than using models of galaxy formation and galactic dust to predict the number and luminosity of such sources.

Neither those models nor pre-FIRAS observations (see Eales et al. 1989) were able to set tight constraints on the presence of Cold Dust. In section 4, we compare our results to those obtained previously.

Our Galactic template spectrum is consistent with detections and upper limits for bright infrared galaxies from the COBE Differential Infrared Background Experiment (DIRBE) (Odenwald, Newmark & Smoot 1995). This is helpful because DIRBE used 140 and 240  $\mu\text{m}$  channels, which IRAS lacks, allowing it to probe significantly cooler dust temperatures than IRAS. DIRBE rules out the possibility of extremely bright sources occurring in the 2% of the high Galactic latitude sky not surveyed by IRAS and sees no evidence for sources whose emission comes predominantly from Cold Dust.

The 1.2 Jy catalog gives redshifts for these galaxies. Most have  $z < 0.05$  and all have  $z < 0.3$ . We take these redshifts into account when fitting to DIRBE fluxes and while extrapolating using the FIRAS spectrum. High redshift galaxies will generate a significant total far-infrared flux and should produce an isotropic cosmic infrared background (Hauser 1995). However, they will be sufficiently distant to lack noticeable clustering on these angular scales and therefore should not produce foreground anisotropy. Toffolatti et al. (1995) found a negligible contribution to anisotropy from non-Poisson fluctuations. Poissonian fluctuations will not lead to anisotropy for distant sources.

### 3. Results

We use the combined FIRAS/DIRBE Galactic spectrum to predict the microwave flux of each IRAS galaxy in Jy ( $1 \text{ Jy} = 10^{-26} \text{ Watt}/\text{m}^2/\text{Hz}$ ). To convert from flux  $S$  to antenna temperature  $T_A$ , we use

$$T_A = S \frac{\lambda^2}{2k_B \Omega} , \quad (1)$$

where  $k_B$  is Boltzmann’s constant,  $\lambda$  is the wavelength, and  $\Omega$  is the effective beam size of the observing instrument. Antenna temperature is related to thermodynamic temperature by

$$T_A = \frac{\frac{h\nu}{k}}{e^{\frac{h\nu}{kT}} - 1} = \frac{x}{e^x - 1} T, \quad (2)$$

defining  $x \equiv h\nu/kT$ . Small fluctuations in antenna temperature can be converted to effective thermodynamic temperature fluctuations using

$$\frac{dT_A}{dT} = \frac{x^2 e^x}{(e^x - 1)^2} . \quad (3)$$

Analysis of source counts indicates that the 1.2 Jy sample is complete down to an extrapolated flux of 3 mJy at 100 GHz. We divide these sources logarithmically into groups of similar flux and find a gradual decrease in anisotropy as flux decreases, showing that dimmer sources will not generate significant anisotropy even if clustered as much as the 1.2 Jy sources. This decrease is consistent with theoretical predictions of fluctuations, which constrain the anisotropy generated by sources too dim to make the 1.2 Jy catalog to be less than 5% of the anisotropy from sources in the catalog. Since these contributions will add in quadrature, temperature anisotropy is dominated by the brightest sources. The contour plot in Figure 2 shows the rms temperature anisotropy of extragalactic infrared sources over the full range of frequencies and instrument resolution (FWHM). The minimum value of  $\frac{\Delta T}{T}$  is  $1.3 \times 10^{-8}$  at large FWHM and medium frequency and the maximum value is 0.092 at small FWHM and high frequency. Our results for temperature anisotropy are fit within about 10% by

$$\log_{10} \frac{\Delta T}{T} = 2.0(\log_{10} \nu)^3 - 8.6(\log_{10} \nu)^2 + 10.3 \log_{10} \nu - 0.98 \log_{10}(FWHM) - 9.2 \quad . \quad (4)$$

The nearly inverse linear relationship between anisotropy and FWHM results from the combined effects of beam convolving and map pixelization. Anisotropy from extragalactic infrared sources dominates expected CMB anisotropy at frequencies above 500 GHz. This makes effective foreground discrimination possible for instruments with a frequency range wide enough to detect the extragalactic infrared foreground fluctuations directly.

The contour plot in Figure 3 shows the results of subtracting pixels where the fluctuations from extragalactic infrared sources are five times greater than the quadrature sum of the rms CMB anisotropy and the expected instrument noise for COBRAS/SAMBA at that frequency (Tegmark & Efstathiou 1995). These  $5\sigma$  pixels can be assumed to contain bright point sources. This plot is best suited for comparison with previous results (Toffolatti et al. 1994, Francheschini et al. 1989) which used  $5\sigma$  subtraction. The  $5\sigma$  subtraction has a significant effect for small FWHM at frequencies below 500 GHz. Galaxies which would be at their brightest at high frequencies fail to reach the  $5\sigma$  threshold there because the expected instrument noise increases rapidly above 500 GHz, although the contribution to  $\sigma$  from CMB temperature fluctuations is decreasing. Real observations of temperature anisotropy will be sensitive to the exact noise spectrum of the instrument. The maximum effect here is to subtract 0.002% of the pixels, leading to a factor of 5 reduction in temperature anisotropy due to IRAS sources. This is further evidence that temperature anisotropy from extragalactic infrared sources is dominated by the brightest sources, suggesting that knowledge of individual bright sources is desirable. The bright sources are a mixture of Local Group galaxies and more distant infrared-luminous galaxies such as starburst galaxies. Optimal subtraction of the extragalactic infrared foreground would avoid eliminating  $5\sigma$  pixels and would instead model the bright sources individually

to predict their microwave fluxes.

#### 4. Conclusions

The recently obtained spectral knowledge of our Galaxy has enabled us to take into account the possible presence of Cold Dust. It is difficult to distinguish dust colder than 10K from the CMB using spectral analysis, but if Cold Dust is accompanied by Warm Dust in all infrared galaxies we can overcome this spectral similarity. The DIRBE upper limits on bright infrared galaxies at 140 and 240  $\mu\text{m}$  argue against the existence of sources whose emission is dominated by Cold Dust. This gives us confidence that other infrared-bright galaxies have a spectrum similar to the Milky Way.

Although subject to systematic errors on a galaxy-by-galaxy basis, we expect our overall results to be accurate to about 20% at high frequencies where galactic dust is bright and will have a significant effect on measurements of CMB anisotropy. At lower frequencies where the CMB fluctuations are dominant and where the amount of synchrotron and free-free emission is appreciable but uncertain, we trust our results to within a factor of two. Our expected level of temperature anisotropy makes the extragalactic infrared foreground dominant over the Galactic foregrounds of dust, free-free, and synchrotron for angular resolutions near  $10'$  and frequencies above 100 GHz. Below 100 GHz, radio sources are expected to be the dominant extragalactic foreground.

Our results agree closely with those generated for sub-degree angular resolution by Toffolatti et al. (1995) with their model of moderate cosmological evolution of all galaxies. Our predictions for anisotropy are lower by about a factor of three than those of Francheschini et al. (1989), who assume strong cosmological evolution of the brightest IR sources and include early galaxies with heavy starburst activity. Wang (1991) ignores

the possibility of cold dust and uses galaxy evolution models to predict anisotropy levels somewhat lower than those found with our phenomenological approach.

Despite the likely presence of Cold Dust in infrared-bright galaxies, our results leave room at intermediate frequencies for the measurement of CMB anisotropies without crippling interference from extragalactic infrared sources. Figure 4 shows a summary of our results for several instrument resolutions. The extragalactic infrared foreground will not be significant around 100 GHz but will be dominant above 500 GHz.

## 5. Acknowledgments

We wish to thank Michael Strauss and Dave Schlegel for their assistance with the IRAS 1.2 Jy catalog. The DIRBE integrated fluxes of the Milky Way were graciously provided by Ned Wright and Janet Weiland. We also thank Bill Reach for supplying the FIRAS Galactic Dust spectrum, Marc Davis, Giovanni DeAmici, and Laura Cayon for helpful conversations, and Joe Silk and Ted Bunn for reviewing a draft of this paper. E.G. acknowledges the support of an NSF Graduate Fellowship. This work was supported in part at LBNL through DOE Contract No. DE-AC03-76SF00098.

## REFERENCES

- Banday, A.J. et al. 1996, submitted to ApJL, astro-ph/9601064
- Bennett, C.L. et al. 1992, ApJ, 396, L7
- Block, D.L., et al. 1994, A&A, 288, 383
- Chini, R., & Krugel, E. 1993, A&A, 279, 385
- Chini, R., et al. 1995, A&A, 295, 317
- Condon, J.J. & Broderick, J.J. 1991, AJ, 102, 1663
- Crawford, T. et al. 1995, ApJ, in press, astro-ph/9511069
- Devereux, N.A. & Young, J.S. 1992, AJ, 103, 1536
- Eales, S.A., Wynn-William, C.G. & Duncan, W.D. 1989, ApJ, 339, 859
- Fisher, K.B., et al. 1995, ApJS, 100, 69
- Franceschini, A., & Andreani, P. 1995, ApJ, 440, L5
- Franceschini, A., Toffolatti, L., Danese, L., & De Zotti, G. 1989, ApJ, 344, 35
- Hauser, M.G. 1995, Proceedings of IAU Symposium 168, “Examining the Big Bang and Diffuse Background Radiations”
- Kogut, A., et al. 1996, submitted to ApJ, astro-ph/9601060
- Kogut, A., et al. 1994, ApJ, 433, 435.
- Neininger, N. & Guelin, M. 1996, in press, astro-ph/9603005
- Odenwald, S., Newmark, J. & Smoot, G. 1995, ApJ, in press
- Reach, W.T. et al. 1995, ApJ, 451, 188
- Rowan-Robinson, M. 1992, MNRAS, 258, 787
- Smoot, G.F. et al. 1992, ApJ, 396, L1

Smoot, G.F. et al. 1995, *Astrophys. Lett.*, 32, 297

Tegmark, M. & Efstathiou, G. 1995, submitted to *MNRAS*, astro-ph/9507009

Toffolatti, L. et al. 1995, *Astrophys. Lett.*, 32, 125

Wang, B. 1991, *ApJ*, 374, 465

Wright, E.L. et al. 1991, *ApJ*, 381, 200

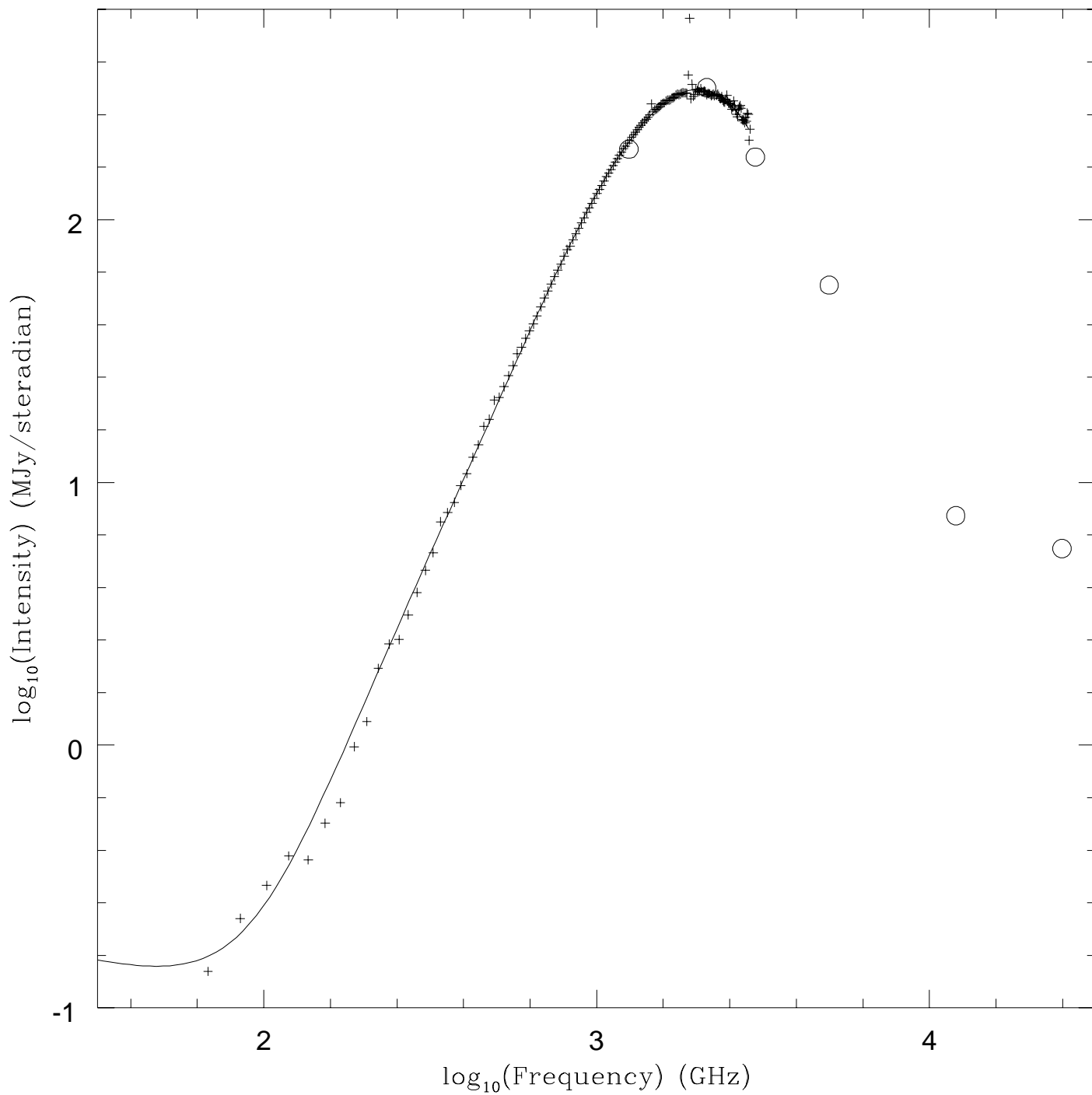
Fig. 1.— The FIRAS Galactic Dust spectrum, including emission lines, is shown by + symbols. The smooth curve is a fit to this spectrum based upon a two-component dust model with synchrotron and free-free emission included. With a  $\nu^2$  emissivity law assumed, the fit is Warm Dust at 19.4K and Cold Dust at 4.3K with an optical depth 12.1 times that of the Warm Dust. The FIRAS error bars are not shown because they are extremely small on this scale. The open circles are DIRBE integrated Galactic fluxes at 12, 25, 60, 100, 140, and 240  $\mu\text{m}$ , normalized to the FIRAS measurements.

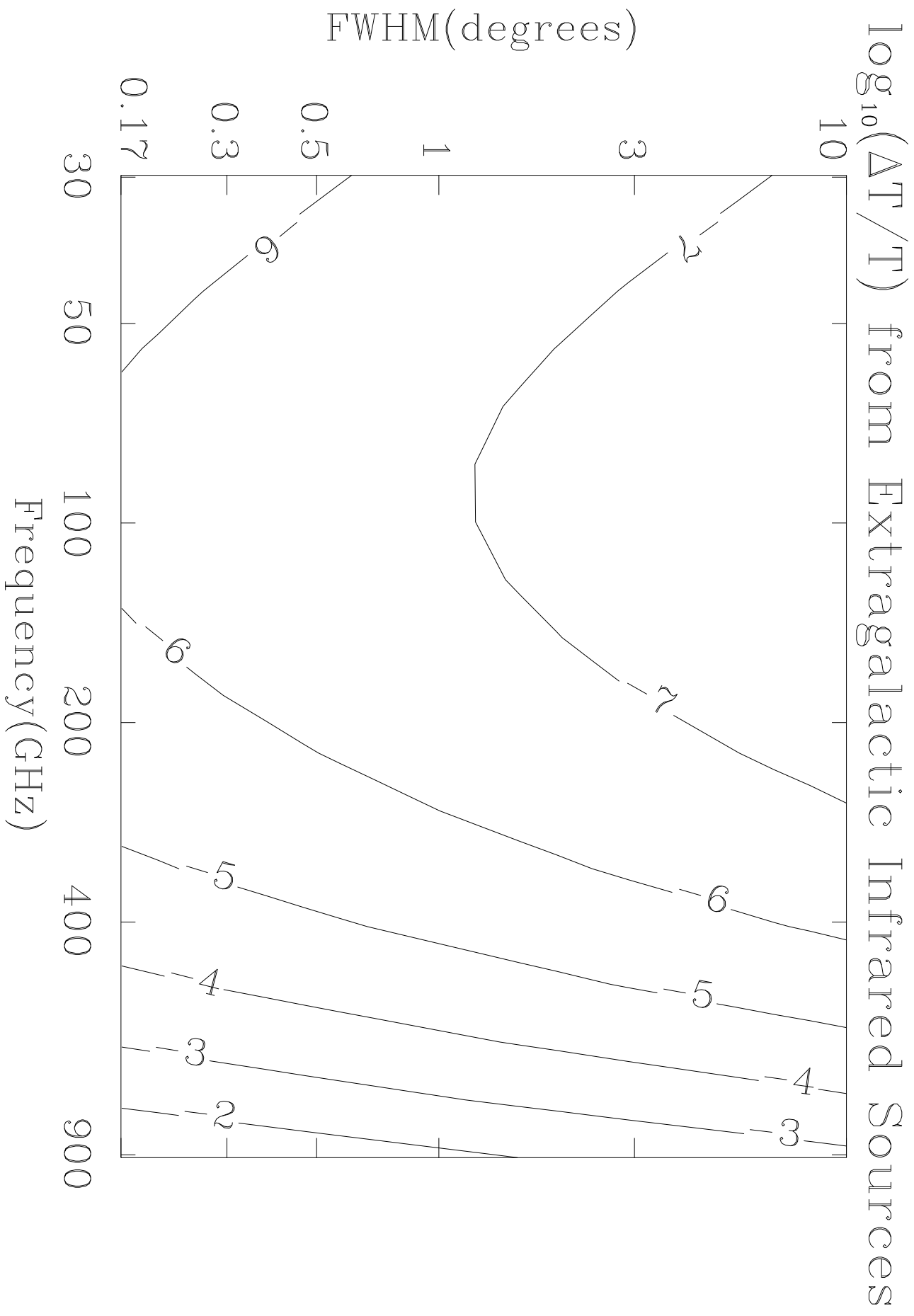
Fig. 2.— A log-log-log contour plot of equivalent thermodynamic temperature anisotropy due to extragalactic infrared sources as a function of frequency in GHz and resolution (FWHM) in degrees. The temperature anisotropy shown is  $\log_{10} \frac{\Delta T}{T}$  where  $\Delta T$  is the root mean square equivalent thermodynamic temperature generated by extragalactic infrared sources in Kelvin and  $T$  is the temperature (2.73K) of the CMB. The increase in anisotropy at low frequencies occurs because synchrotron and free-free emission are included in our template spectrum.

Fig. 3.— A log-log-log contour plot of our results with pixels at a level of  $5\sigma$  removed. This decreases the level of anisotropy for small beam sizes where more bright sources reach the  $5\sigma$  cutoff.

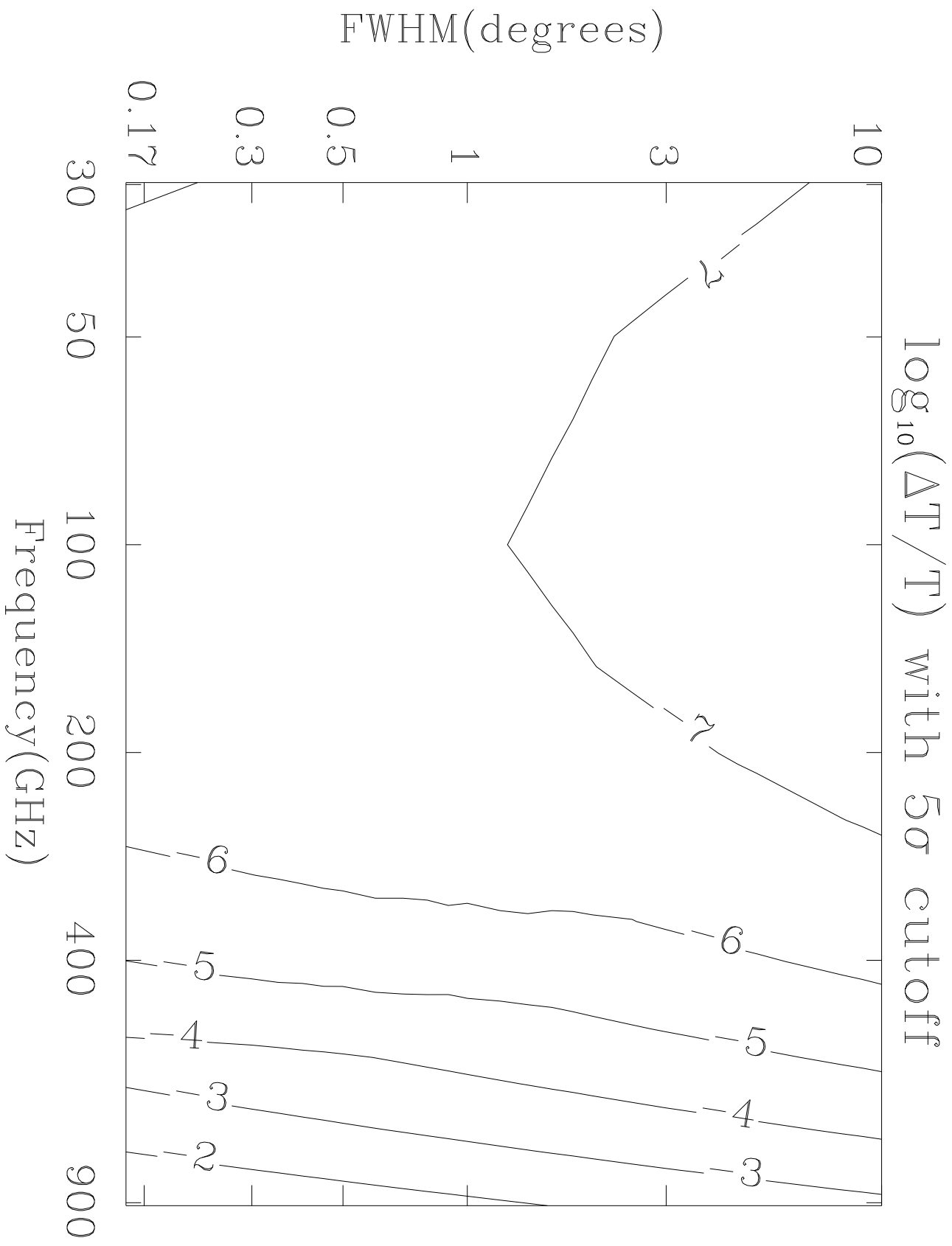
Fig. 4.— Plot of  $\log_{10} \frac{\Delta T}{T}$  (with no pixels subtracted) versus frequency for instrument resolutions of  $10'$ ,  $30'$ ,  $1^\circ$ , and  $10^\circ$ , showing window where foreground confusion should be less than  $10^{-6}$ .

Galactic Far-infrared Emission Spectrum











# Confusion from Foreground Anisotropy

